Supporting Information

Unravelling the white light emission in the single-phase new stochiometric vanadate phosphor synthesized by the rapid low-temperature one-pot synthesis and its W-LED prototype with high CRI and luminous efficacy

*Asish K. Dehury[a, b], Manas K. Sahoo[a], Rajeswari Kainda[a, b], and Yatendra S. Chaudhary[a, b]**

[a]Materials Chemistry Department, CSIR-Institute of Minerals and Materials Technology, Bhubaneswar, 751013, India

[b]Academy of Scientific and Innovative Research (AcSIR), Ghaziabad - 201002, India

**Email: yschaudhary@immt.res.in*

Experimental Section

Materials

Barium nitrate (99.999% trace metals basis), Sodium metavanadate (≥98.0%), and Potassium hydroxide (anhydrous, ≥99.95% trace metals basis) purchased from Sigma Aldrich were used without any further purification. Milli-Q deionized water was used for synthesis and the washing process.

Phosphor Synthesis

In a typical synthesis of $Ba_3V_4O_{13,}$ stoichiometric amounts $Ba(NO_3)_2$ and $NaVO_3$ were dissolved in 2 ml milli q water each and taken separately in separate beakers. As $NaVO_3$ was not completely dissolved in water, the solution was heated for 5 min at 80°C. $Ba(NO_3)_2$ solution was added dropwise to $NaVO_3$ solution to get a reaction mixture and stirred for 30 min. 6M KOH was used as a mineralizer to maintain a pH value of nearly 12.5, and instantly, a precipitate was formed, which was then transferred to the microwave-reactor vessel for microwave synthesis (Anton Paar Monowave-400). The pressure of the reaction medium was varied from 11.1 to 13.5 mbar and synthesized at 180, 200 & 220°C t and for 5-, 10-, 15-, 30-, 45- & 60- min reaction time. After the completion of the synthesis, the product was separated from the reaction solution using a centrifuge at 10000 rpm for 5 min followed by washing

with water until neutral pH was achieved. The resulting products were dried in an air oven at 80^{o}C for 6 h. The pale white product was obtained, which was kept for future use. The synthesis yield calculated for obtained phosphors is approximately 90%.

Prototype White LED Device Fabrication

A white LED device prototype was fabricated by combining a 350 nm UV LED chip (Ktron India Pvt. Ltd) with the synthesized single-phase phosphor. The phosphor was mixed in a 1:1 ratio with silicone resin (Dow Europe GmBH) and then packaged onto the surface of the UV LED chip. A spectrometer system (Oceanview optics) was utilized to determine the photoelectric properties (Emission spectrum, CCT, CRI, luminous efficacy) of the as-fabricated white Light emitting device.

Structural and Morphology Characterization

The crystallinity of the synthesized samples was confirmed from an X-ray diffractometer (X'PERT PANalytical) using Cu Kα radiation (λ = 1.5046 Å) in the 10−90° 2θ range with scan speed of 2°/min and 0.02° steps. The morphology evolution of synthesized samples was evaluated on a field emission scanning electron microscope (FESEM) (JEOLJSM Model: 6510, Japan) and high-resolution transmission electron microscope (HRTEM) (Joel-JEM-F200) with the facility to get the lattice fringes and SAED patterns. The elemental composition analysis and mapping were carried out with an energy-dispersive X-ray spectrometric system (EDAX) attached to the FESEM instrument. Fourier Transfer Infrared Spectroscopy (FT-IR) was performed in Perkin Eleimer Frontier. Raman studies were done using a Renishaw in Via micro-Raman spectrometer in the back-scattering geometry with a 1064 nm Nd: YAG laser as an excitation source. XPS measurements were carried out using multi-chamber XPS (PREVAC, Poland), and Electron paramagnetic resonance (EPR) was performed using a Bruker BioSpin AG spectrometer to confirm the presence of paramagnetic species and, hence, the unpaired electrons in the phosphor.

Emission and Underlying Mechanism

To elucidate the optical properties of the materials UV-Vis DRS and photoluminescence (PL) spectroscopy were performed. The DRS was examined using a UV-Vis spectrophotometer (UV-2450 SHIMADZU). The photoluminescence emission spectra, CIE, and Photoluminescence quantum efficiency (PLQE) were recorded using an Edinburg F980s spectrometer. Time-resolved photoluminescence (TRPL) measurements were performed, and decay profiles were analyzed by nonlinear least-squares iteration procedures using FLS980 decay analysis software, keeping the chi-square (χ^2) values near one and uniform distribution of residuals. The temperature-dependent (cryo-) PL and fluorescence were examined using a Horiba Fluorolog-QM fluorescence spectrophotometer equipped with a closed-cycle liquid nitrogen cryostat and a digital temperature controller. These measurements were performed at ambient conditions and room temperature using as-synthesized power samples.

Model System and Computational Methods

FullProf software was used to perform Rietveld refinement using the XRD spectra as an input file. The computations were performed using the CRYSTAL17, which applied the density functional theory (DFT) framework and the B3LYP hybrid function. The scheme characterizes the Ba, V, and O centers as 86-411d41G, 86-411d41G, 97-641d51G, and 6-31G*, respectively. The CRYSTAL Resources Page 47 defines core and valence electrons for the valence basis set that represents the Ba, V, and O centers. The Fock matrix was diagonalized using k-point grids in reciprocal space, with a Pack−Monkhorst/Gilat shrinkage factor of IS = ISP = 4. The accuracy thresholds for calculating Coulomb and exchange integrals were set to 10−7 (ITOL1 to ITOL4) and 10−14 (ITOL5), respectively. Additionally, the proportion of Fock/Kohn−Sham matrices mixing was adjusted to 40 (IPMIX = 40). The band structures were acquired by traversing the relevant high-symmetry routes of the Brillouin zone. It is essential to be cautious in this matter. It is widely recognized that DFT tends to underestimate the band gap value. Although hybrid functional and dynamical mean field theory have been tried to address the issue, it is still reasonable to employ DFT with the Becke 3-parameter (exchange) and Lee-Yang-Parr (B3LYP)

functional. The initial geometry was obtained from XRD experimental results, considering the removal of O atoms in this system through the option provided by the CRYSTAL program.

Table S1. The detailed analysis and crystal parameters

Formula	$Ba_3V_4O_{13}$
Radiation	Cu kα
2θ range	10-90
Symmetry	monoclinic
Space group	C 2/c
a (Å)	16.1071(19)
b (Å)	8.94937(20)
c (Å)	10.1714(8)
α (º)	90
β (º)	114.4384(26)
γ (º)	90
Volume($Å^3$)	1334.83(4)
R_p	2.540
R_{wp}	5.429
χ^2	5.741

Table S2. Refined atomic coordinate parameters data at room temperature.

label	**element**	**multiplicity**	**x**	**y**	**z**	**frac**	**U_{iso}**
O2	O-2	8	0.163056	0.674751	0.444167	1	0.006
O6	O-2	8	0.144094	0.127792	0.676071	1.063	0.0196
Ba2	Ba+2	4	0	0.117731	0.75	0.976	0.005
Ba1	Ba+2	8	0.294524	0.66312	0.301952	0.958	0.003
O3	O-2	8	0.165395	0.451451	0.271957	1.214	0.0409
O7	O-2	4	0	0.559835	0.25	1.081	0.0241
O4	O-2	8	0.128051	0.079045	0.39941	1	0.0087
O5	O-2	8	-0.02105	0.173346	0.454638	1.055	0.0141
O1	O-2	8	0.126464	0.377968	0.507441	1.036	0.0111
V2	V+5	8	0.114151	0.511863	0.368384	0.947	0.001
V1	V+5	8	0.091721	0.188511	0.50259	1.006	0.0056

Table S3 Bond distance and bond angles of the distorted lattice of BVO-200-30.

Cluster	Bond/Angle	Value
	V1-O5	1.68800 Å
	V1-O1	1.77977 Å
	V1-O4	1.70639 Å
	V1-O6	1.69966 Å
	V2-O1	1.80101 Å
	V2-O2	1.68448 Å
	V2-O3	1.61400 Å
	V2-O7	1.78406 Å
VO_4	O6-V1-O6	106.748^{O}
	O2-V1-O4	112.314 ^{O}
	O6-V1-O4	107.804 ^{O}
	O4-V1-O5	112.319 ^{O}
	O1-V2-O3	109.666 ^{O}
	O3-V2-O7	108.288 ^{O}
	O2-V2-O3	107.942 ^{O}
	O7-V2-O2	104.886 ^{O}
	V2-O7-V2	152.152 ^{O}
	V1-O1-V2	132.911 ^{O}

Table S4. CIE coordinated at different excitation wavelengths for BVO-200-15

λ_{ex}	CIE
290	(0.302,0.344)
300	(0.316,0.353)
310	(0.323,0.358)
320	(0.328,0.360)
330	(0.330,0.362)
340	(0.331,0.365)
350	(0.333,0.368)
360	(0.336,0.372)
370	(0.341,0.380)

Table S5. CIE coordinated at different temperatures for BVO-200-15

Temp	CIE(X, Y)
20°C	(0.333,0.368)
40°C	(0.331,0.366)
60°C	(0.330,0.363)
80°C	(0.330,0.361)
100°C	(0.329,0.360)
120°C	(0.328,0.358)
140°C	(0.327,0.357)
160°C	(0.325,0.353)
180°C	(0.323,0.351)
200°C	(0.321,0.345)
220°C	(0.319,0.343)
240°C	(0.315,0.341)
260°C	(0.272,0.336)

Table S6 The CIE, CCT, CRI, Luminous Efficacy(LE), Applied Current(I), and UV source wavelength for the current work and other reported better-performing phosphor

Sl No.	Material	CIE	CCT (K)	CRI	LE (lm/W)	I (mA)	λ_{ex} (nm)	Ref.
1	$Ba_3V_4O_{13}$	(0.333,0.368)	5563	86.1	128.4	20	365	**This work**
2	$Ca_2KZn_2(VO_4)_3$	Yellow-green	5349	84.3	-	-	385	1
3	$Cs_2SnCl_6:Bi^{3+}/Te^{4+}$	(0.339,0.365)	5233	81	-	25	-	2
4	Cs_3ZnI_5:Mn	(0.30, 0.38)	6530	78			-	3
5	$CSVO_3$	(0.305,0.420)	6311	62.8	48.2	50	-	4
6	$CSVO_3$:Rb	(0.334,0.443)	5481	62.0	115.8	20	-	5
7	KVO_3	(0.362,0.453)	4859	73	-	-	-	6
8	$RbVO_3$	(0.316,0.424)	5,993	70	-	-	-	6
9	BCNO	(0.318,0.476)	-	-	-	-	-	7
10	$Cs_2Cd_2BrCl_5$	(0.382,0.436)	4286	84.6	-	-		8
11	$Cs_3Cu_2Br_5$:Pb NCs	(0.333,0.341)	5,469	98	1.2	7.8	-	9
12	$CsCu_2I_3$	(0.345,0.364)	5,035		-	-	-	10
13	$Cs_2InCl_5 \cdot H_2O:Sb^{3+}$	(0.358,0.355)	4,556	86		20	-	11
14	$Cs_2Ag_{0.60}Na_{0.40}InCl_6$	(0.396,0.448)	4,054	-	-	-	-	12
15	$Ba_2[Sn(OH)_6][B(OH)_4]_2$	(0.42, 0.38)	3083	94.1	-	-	-	13
16	$Rb_2CdCl_2I_2$	(0.39, 0.41)	-	88	-	-	-	14
17	$Sr_{10}V_6O_{25}$	(0.30,0.35)	-	-	-	-	-	15
17	$Ca_{10}V_6O_{25}$	(0.350,0.368)	-	-	-	-	-	16
17	$Ba_3V_2O_8$	(0.353,0.392)	4867	85	102	140	365	17
18	Cu doped ZnS	(0.351,0.398)	4538	97	-	-	310	18

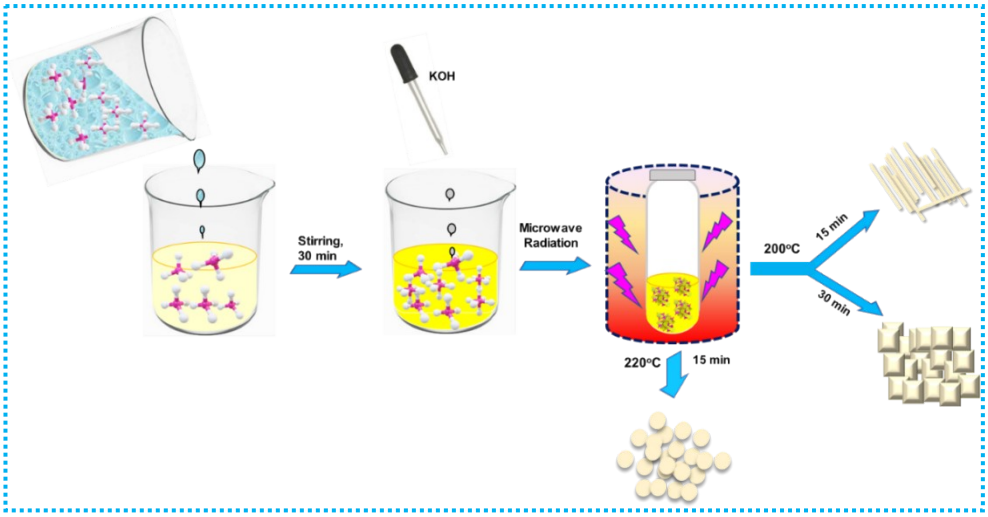

Fig. S1 Synthesis route of microwave-assisted synthesis showing tuning of morphology with reaction condition

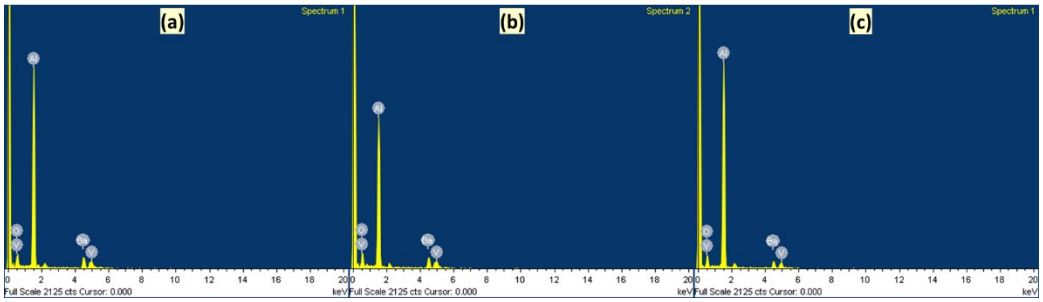

Fig. S2 EDAX of (a) BVO-200-15 (b) BOV-200-30 (c) BVO-220-15

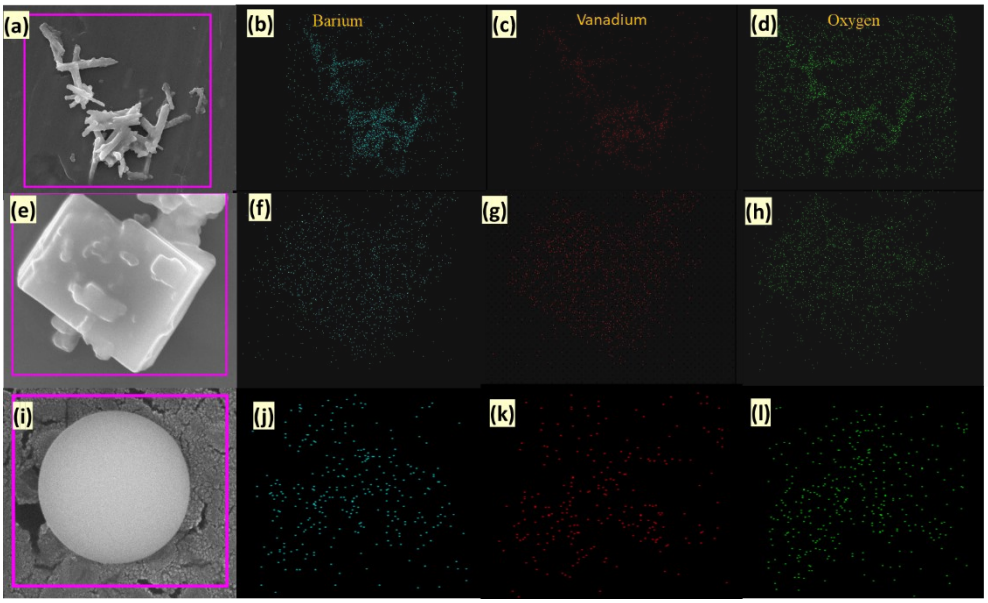

Fig. S3 Elemental Mapping of (a-d) BVO-200-15 (e-h) BVV-200-30 (i-l) BVO-220-15

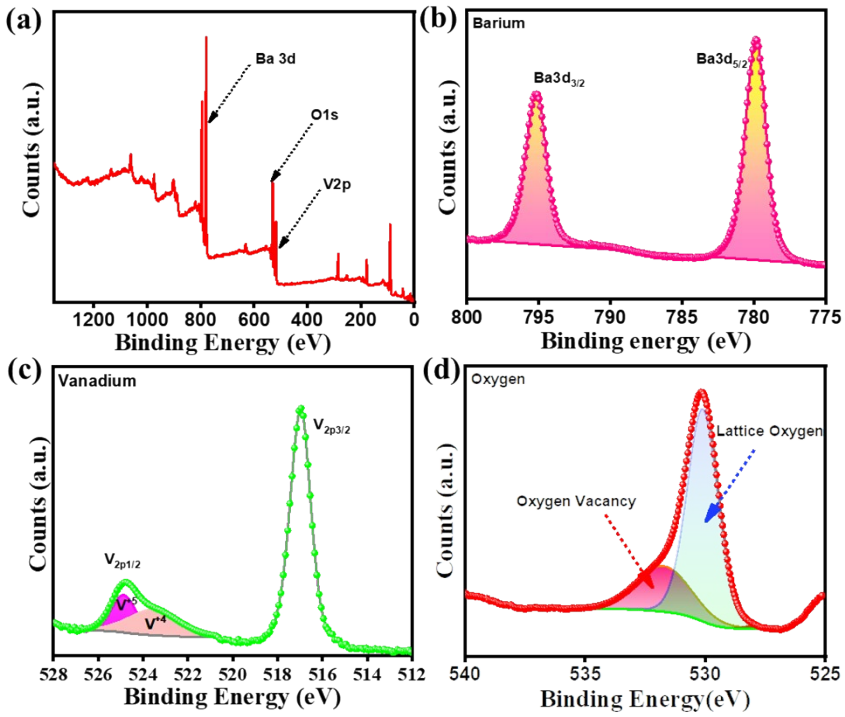

Fig. S4. (a) XPS survey scan **(b)** Barium, **(c)** Vanadium, and (d)Oxygen of BVO-200-30

Supporting References

1. L. Bharat, S. K. Jeon, K. Krishna and J. S. Yu, *Sci. Rep*., 2017, **7**, 42348.
2. Z. Wei, Z. Wei, L. Lingyun, H. Ping, G. Zhongliang, Z. Ziwei, S. Jinyue, Y. Yan and C. Xueyuan, *Angew. Chem. Int. Ed.,* 2022, **61**, e202116085.
3. B. Ramavath, L. F. Iago, P. Seelam and P. Lakshminarayana, *ACS Appl. Mater., Interfaces* 2023, **15**, 35206−35215.
4. N. Tomohiko, I. Masahiko, U. Yuko and T. Tetsuo, *J. Mater. Chem. C,* 2015, **3**, 10748-10754.
5. E. Pavitra, R. G. Rama, L. K. Bharat, J. Y. Park, C. H. Kwak, J. W. Chung, Y. K. Han and Y. S. Huh, *J. Mater. Chem. C,* 2018, **6**, 12746—12757.
6. T. Nakajima, M. Isobe, T. Tsuchiya and Y. T. Kumagai, *Nat. Mater*., 2008, **7**, 735–740.
7. O. Takashi, K. Yutaka, I. Ferry, W. Wei-Ning and O. Kikuo, *Adv. Mater.,* 2008, **20**, 3235–3238.
8. H. Xu, X. Dong, Z. Zhang, L. Huang, H. Zeng, Z. Lin and G. Zou*, J. Mater. Chem. C,* 2022, **10**, 13844

9. S. Zhao, S. Jiang, W. Cai, R. Li, Q. Mo, B. Wang and Z. Zang, *Cell Rep*., 2021, **2**, 100585.
10. R. Lin, Q. Guo, Q. Zhu, Y. Zhu, W. Zheng and F. Huan, *Adv. Mater*., 2019, **31**, 1905079.
11. Y. Jing, Y. Liu, X. Jiang, M. S. Molokeev, Z. Lin and Z. Xia, *Chem. Mater*., 2020, **32,** 5327-5334.
12. J. Luo, X. Wang, S. Li, J. Liu, Y. Guo, G. Niu, L. Yao, Y. Fu, L. Gao, Q. Dong, C. Zhao, M. Leng, F. Ma, W. Liang, L. Wang, S. Jin, J. Han, L. Zhang, J. Etheridge, J. Wang, Y. Yan, E. H. Sargent and J. Tang, *Nature*, 2018, **563**, 541.
13. Y. Lin, G. E. Wang, C. L. Hu, J. H. Feng, L. N. Li and J. G. Mao, *Angew. Chem. Int. Ed.,* 2019, **58**, 13390 –13393.
14. X. Li, S. Wang, S. Zhao, L. Li, Y. Li, B. Zhao, Y. Shen, Z. Wu and P. Shan, L. J. Junhua, *Chem. Eur. J.* 2018, **24**, 9243 – 9246.
15. M. M. Teixeira, A. F. Gouveia, Al. Gama de Sousa, L. Fernando da Silva, R. Cristina de Oliveira, M. A. San-Miguel, M. S. Li and Elson Longo, *J. Phys. Chem. C,* 2020, **124**, 14446-14458.
16. M. M. Teixeira, Y. G. Gobato, L. Gracia, L. F. da Silva, W. Avansi Jr, M. Assis, R. C. de Oliveira, G. A. Prando and J. Andrés, E. Longo, *J. Lumin.,* 2020, **220**, 116990.
17. A. K. Dehury, R. Kainda and Y. S. Chaudhary*, Inorg. Chem.,* 2023, **62**, 17163-17181.
18. A. K. Dehury, S. K. Behera, S. K. Chirauri, S. Basu and Y. S. Chaudhary, *Chem. Asian J.,* 2022, **17**, e202200948.